NASA Contractor Report 3030

Towards Complete Configurations Using an Embedded Grid Approach

Charles W. Boppe

CONTRACT NAS1-14732
JULY 1978

NASA

NASA Contractor Report 3030

Towards Complete Configurations Using an Embedded Grid Approach

Charles W. Boppe
Grumman Aerospace Corporation
Bethpage, New York

Prepared for
Langley Research Center
under Contract NAS1-14732

National Aeronautics
and Space Administration

**Scientific and Technical
Information Office**

1978

TOWARDS COMPLETE CONFIGURATIONS USING AN EMBEDDED GRID APPROACH*

Charles W. Boppe
Grumman Aerospace Corporation

SUMMARY

A new approach to simulating transonic flow about transport configurations is briefly outlined. The method's embedded grid scheme provides a high degree of computational resolution coupled with geometric flexibility for future applications to complex shapes. Calculations presented illustrate aspects of transonic transport design including fuselage design, determination of wing control surface deflection effectiveness, and wing design.

INTRODUCTION

Numerical simulations of transonic flows have experienced considerable development following the success of Murman and Cole (Reference 1). Two-dimensional relaxation schemes for treating simple airfoils evolved to provide methodology for the design and analysis of complex airfoil shapes. Similarly, three-dimensional codes capable of treating simple wing shapes have provided the foundation for codes now used for completely arbitrary wings. At the present time, a number of schemes are available for analyzing simple wing-body shapes at transonic speeds (References 2-6). Efforts are now being directed at the goal of developing methodology for treating complex, realistic wing-fuselage geometries.

A high degree of computational resolution is required if flow details about complex shapes are to be obtained. Providing this resolution for both a wing and fuselage simultaneously presents a difficult problem. In addition, computational mesh flexibility is required to permit the treatment of truly arbitrary shapes. This must all be accomplished with sufficient computing efficiency to insure a cost-effective approach to resolving engineering design problems. These requirements place a severe strain on the conventional single computational grid approach which characterizes existing numerical methods.

Recently, Chen, Tinoco and Yoshihara (Reference 7) proposed a novel approach aimed at solving the aforementioned difficulties. By coupling a three-dimensional transonic relaxation scheme with a subsonic panel method for treating the fuselage, certain problems related to resolution and geometric flexibility are resolved. Providing that transonic flow effects on the fuselage are not required, the approach is shown to provide detailed fuselage interference effects on the wing.

---

* This work was supported by NASA-LRC under Contract NAS1-14732.

This paper briefly describes a new approach for providing both detailed computational resolution for wing-fuselage geometries and computational mesh flexibility for treating the more complex shapes anticipated in future applications. This is accomplished by the implementation of a multiple computational grid approach. Primarily, however, this paper will concentrate on the application of this methodology to certain aspects of transonic transport design. Additional details of the mesh embedding scheme can be found in Reference 8.

SYMBOLS

M_∞	Freestream Mach Number
b	Wing Span
η	2y/b Wing Span Position
δ^*	Boundary Layer Displacement Thickness
α	Angle of Attack
δ_F	Control Surface Deflection
C_p	Pressure Coefficient
C_p^*	Critical Pressure Coefficient
C_ℓ	Section Lift Coefficient
γ	Specific Heat Ratio
φ	Velocity Perturbation Potential
$\Lambda_{c/2}$	Mid-Chord Sweep Angle

APPROACH

Three computational grid arrays are employed to compute the transonic flow about wing-fuselage configurations. Figure 1 is a schematic illustrating the geometry/mesh arrangement. Fine grid arrays are embedded along the wing between the fuselage juncture and the wing tip. A second fine grid system encompasses the entire fuselage. A global crude grid fills the entire computational space in which the configuration along with the body and wing fine grid systems are embedded. The global crude and body fine mesh arrays are Cartesian systems while the wing fine grid is skewed for wing sweep and taper. The velocity potential (φ) is computed at all mesh points in each grid system. Interaction between the three mesh arrays is accomplished by means of grid overlap regions.

Fine grid solutions are computed only in regions very close to the wing and fuselage where gradients are large and details are important. Beyond this, the crude grid treats the remainder of the flow field. The calculations presented herein were made with 100 evenly spaced grid points between the wing leading and trailing edge at each wing span station. Fuselage cross-section cuts are represented with 40 grid points. A total of 4500 boundary points fall on the wing and fuselage surfaces. Computing time on the IBM 370 system is 45 minutes. This would be equivalent to about 15 minutes on the CYBER 175 system or about 9 to 10 minutes on the CDC 7600.

The relaxation scheme is constructed about an extended or modified transonic small disturbance flow equation.

$$\left[1 - M_\infty^2 - (\gamma + 1) M_\infty^2 \varphi_x - \frac{\gamma + 1}{2} M_\infty^2 \varphi_x^2\right] \varphi_{xx} - 2 M_\infty^2 \varphi_y \varphi_{xy} \qquad (1)$$

$$+ \left[1 - (\gamma - 1) M_\infty^2 \varphi_x\right] \varphi_{yy} + \varphi_{zz} = 0$$

Several terms found in the full potential equation have been added to the classical transonic small disturbance equation to improve shock wave resolution for arbitrary swept wings. It should be noted that the grid embedding scheme would not be restricted to a small-disturbance formulation. The simplicity of the small-disturbance planar boundary conditions does, however, facilitate implementation of the basic approach.

A geometry modeling system is employed to convert complex fuselage geometry into suitable fuselage boundary conditions for the body computational surface. This system, developed by Vachris and Yaeger (Reference 9), provides a continuous analytical model of the surface geometry given certain cross-section line and body line input models. Examples of fuselage geometry models are included in the sample calculations which follow.

RESULTS AND DISCUSSION

Wing Control Surface Effectiveness

Experimental results for a supercritical wing, area ruled fuselage transport model were recently reported by Mann and Langhans (Reference 10). The results are of particular interest because they illustrate the effect of control surface deflections on a transport with a supercritical wing when the flow is transonic and shock waves are present. The present method has been employed to determine whether or not control surface deflection effectiveness can be predicted theoretically. This type of computation would be useful both for sizing the wing control surfaces and for loads required to size actuators.

The configuration can be seen in Figure 2. The aspect ratio 7.5 wing has a quarter chord sweep of 33°. The taper ratio is 0.4 with thickness varying between 11% at the root to 6% at the tip. The configuration is designed for a lift coefficient of 0.5 at a Mach number of 0.9. Experimental data are presented in Reference 10 for four different control surfaces at various positions along the wing span. Control surface number 2 has been selected for correlations since its effect on pressure distributions and shock wave pattern is the greatest. Comparisons are made at a station located on the control surface and at stations on either side of the control surface (see Figure 2).

Fuselage contours for this area ruled test model can be seen in Figure 3. In addition, this figure illustrates the construction of the body surface mathematical model. The Quick-Geometry model is constructed using key input body line and cross-section line models. In this case, body lines include the body top centerline, bottom centerline and max-half-breadth line. They are defined by cubics, lines and ellipses along with their specified ranges of applicability. Cross-section line models are specified using body lines as limiters. The fuselage illustrated is constructed using only one cross-section model and three body line models.

A wing boundary layer displacement thickness has been computed by coupling a two-dimensional transonic viscous analysis (Reference 11) with simple sweep theory. Wing sections are extracted at several stations along the span. Section ordinates are scaled by the cosine of the mid-chord line sweep angle. Similarly, airfoil flow conditions are given by

$$M_{2\text{-}D} = M_{\infty} * \cos \Lambda_{c/2} = 0.77 \tag{2}$$

$$C_{\ell_{2\text{-}D}} = \frac{C_{\ell\ 3\text{-}D}}{\cos^2 \Lambda_{c/2}} = 0.72 \tag{3}$$

for the $\eta = 0.31$ span station illustrated in Figure 4 where the wing section lift coefficient is approximately 0.53. The computed airfoil δ^* is then rescaled for the wing streamwise sections and added to the wing geometry on both the upper and lower surfaces. Displacement thicknesses for both the basic wing and wing with control surface deflected can be seen in Figure 4. Unfortunately, flow separation was indicated at 36% chord on the deflected section upper surface and 87% chord on the lower surface. As a result, the experimental flow may not be completely attached. These comparisons are still thought to be instructive although this possibility must be noted. This procedure provides a fast, inexpensive means for obtaining an approximation to the viscous effects of the three-dimensional wing.

Correlations with experimental data for the basic wing can be seen in Figure 5. Figure 6 is a similar set of comparisons for the wing with control surface number 2 deflected upward 15°. These figures illustrate both severe spanwise variations in flow characteristics and the effect of control surface deflection. Results presented in Figure 6 indicate that the attached flow theory predicts a slightly stronger control surface effect than that indicated by the experimental data. This is probably attributable to a flow separation region on the wing upper surface. It is likely that the flow has reattached itself to the wing at some position before the trailing edge. Viscous theories capable of treating this type of flow field are currently under development. Still, however, it can be seen that the attached flow analysis predicts the basic character of the wing flow field when a control surface is deflected.

Wing Design

A supercritical wing transport configuration which was recently designed and tested at Grumman can be seen in Figure 7. This wing has an aspect ratio of 8.55 and a sweep of 27° at the quarter-chord line. Wing thickness ($11\frac{1}{2}\%$) is constant across the entire span. The engine pods are included in this figure for illustrative purposes. They are not included in the analysis or experimental data presented.

Superimposed computed pressure distributions for the wing upper surface can be seen in Figure 8 for the condition $M_\infty = 0.825$, $\alpha = 4°$. The lift coefficient for this case is approximately 0.5. The Mach number is higher than the design Mach of 0.80 to provide a case with an appreciable shock wave. Correlations with experimental data at four span stations can be seen in Figure 9. Correlation is good across the entire span except for a discrepancy near the leading edge of the highly swept glove region.

Details of the wing mid-span pressure distribution can be seen in Figure 10 along with the streamwise wing section. The fine embedded wing grid provides 100 evenly spaced mesh points between the leading and trailing edge of each section. The mesh is evenly spaced so that a shock wave will be resolved to an equivalent degree independent of its position along the wing chord.

The drag force acting on wing-fuselage configurations at transonic speeds cannot be predicted with any degree of accuracy or reliability using the present inviscid method. This would also be true for methods currently employing the full potential equation and exact boundary conditions. This should not be surprising. The work of Bob Melnik at Grumman indicates that the accurate prediction of airfoil drag in two dimensions has been made possible only recently. This requires the incorporation of a sophisticated viscous analysis which includes not only the effects of wing boundary layer displacement thickness, but also the important effects of wake curvature. In all probability, it will be a number of years before this type of capability is available for three-dimensional flows.

This methodology can play a role in wing design at the present time although computed drag forces may not be used directly. At Grumman it has been found advantageous to design transonic wings by first designing a two-dimensional airfoil. Airfoil design conditions are provided by sweep theory. A preliminary wing design is obtained by coupling the design airfoil with camber and twist distributions given by an inexpensive subsonic panel method. Total drag is constructed from friction and wave drag components provided by the two-dimensional analysis and the lift-induced component provided by the three-dimensional analysis. More important, however, the three-dimensional analysis indicates how close the wing pressure distributions match that of the designed airfoil. In particular, the designer can discover shock wave unsweeping, usually an indication that a problem exists, long before the first wind tunnel test.

Fuselage Design

Computed fuselage pressure distributions for the supercritical wing transport configuration can be seen in Figure 11. This figure illustrates a computational capability for predicting both effects caused by body contours and wing lift carry-over. This figure also indicates that difficult design problems exist for fuselage geometries as well as wings. At transonic speeds, flow accelerations over the canopy region can lead to shock waves which may cause fuselage flow separation.

The present method is particularly well suited to treat fuselage flow details. This is made possible by combining the flexibility of the geometry modeling system with the detailed mesh resolution of the grid embedding technique. Figure 12 illustrates the fuselage geometry model employed for the aforementioned transport configuration. In addition to providing detailed resolution for fuselage shapes and wings in general, the grid embedding scheme can be used to obtain intense resolution in a very small region that would be of particular interest. In this case, the fine mesh region is concentrated about the nose, windshield, and canopy region of the fuselage. This is done to provide details of this region's flow to permit recontouring of the fuselage lines which would result in a weakening of the canopy shock wave.

Fortunately, the fuselage math model is analytic in nature and continuously defined. As a result, one geometry model can be used for both crude and fine grid systems. The geometry for the fine grid region can be seen in Figure 13. Cross sections are represented with 40 mesh points each at approximately 50 stations in the axial direction between the nose and back end of the canopy.

Correlations with experimental data for the fuselage nose shape can be seen in Figure 14. Correlation is good even though no attempt has been made to incorporate viscous effects in this case.

CONCLUDING REMARKS

A computational method has been described which provides a high degree of resolution for both wing and fuselage shapes simultaneously. In addition, applications to current aircraft design problems have been noted. Future work will take advantage of the mesh flexibility inherent in the grid embedding approach. The treatment of body and wing shapes is currently in hand. The simplicity of planar boundary conditions and Cartesian coordinate arrays make it possible to extend this methodology for the treatment of very complex aircraft configurations. Aircraft components such as winglets, pylons, and pods (see Figure 15) will be modeled within their own grid system. These components will then be combined in the same manner that configurations are modeled with surface singularities in subsonic panel methods. In this form the full potential of the present approach will be obtained.

REFERENCES

1. Murman, E. M. and Cole, J. D., "Calculation of Plane Steady Transonic Flows," AIAA Journal, 9, 1971.

2. Bailey, F. R. and Ballhaus, W. F., "Comparisons of Computed and Experimental Pressures for Transonic Flows About Isolated Wings and Wing-Fuselage Configurations," NASA SP-347, March 1975, pp. 1213-1231.

3. Albone, C. M., Hall, M. G. and Joyce, G., "Numerical Solutions For Transonic Flows Past Wing-Body Combinations," Symposium Transsonicum II, Göttingen, Germany, September 1975.

4. Jameson, A. and Caughey, D. A., "Finite Volume Method For Transonic Potential Flow Calculations," AIAA Paper 77-635, June 1977.

5. Schmidt,W. and Vanino, R., "The Analysis of Arbitrary Wing-Body Combinations in Transonic Flow Using a Relaxation Method," Symposium Transsonicum II, Göttingen, Germany, September 1975.

6. Klunker, E. B. and Newman, P. A., "Computation of Transonic Flow About Lifting Wing-Cylinder Combinations," Journal of Aircraft, Volume II, No. 4, April 1974.

7. Chen. A., Tinoco, E. and Yoshihara, H., "Transonic Computational Design Modifications of the F-111 TACT," AIAA Paper 78-106, January 1978.

8. Boppe, C. W., "Computational Transonic Flow About Realistic Aircraft Configurations," AIAA Paper 78-104, January 1978.

9. Vachris, A. F. and Yaeger, L. S., "Quick-Geometry - A Rapid Response Method for Mathematically Modeling Configuration Geometry," NASA SP-390, October 1975, pp. 49-73.

10. Mann, M. J. and Langhans, R. A., "Transonic Aerodynamic Characteristics of a Supercritical-Wing Transport Model with Trailing-Edge Controls," NASA TMX-3431, October 1977.

11. Bauer, F., Garabedian, P., Korn, D. and Jameson, A., Supercritical Wing Sections II, Springer-Verlag, New York, 1975.

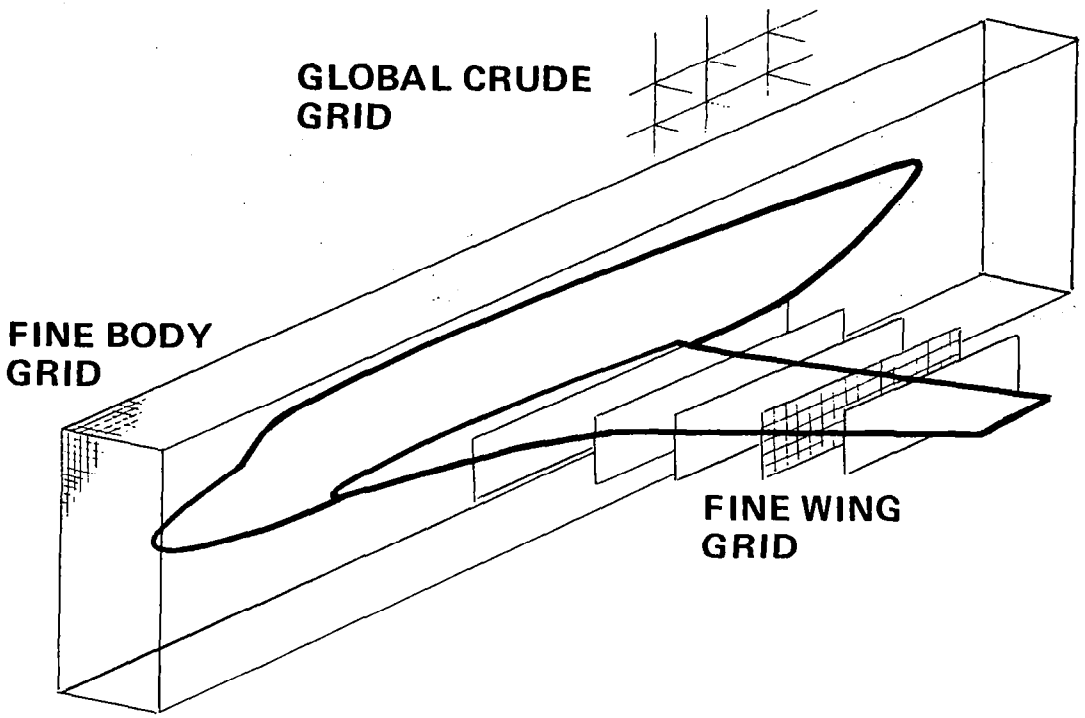

Figure 1.- Wing-fuselage configuration with computational mesh arrangement.

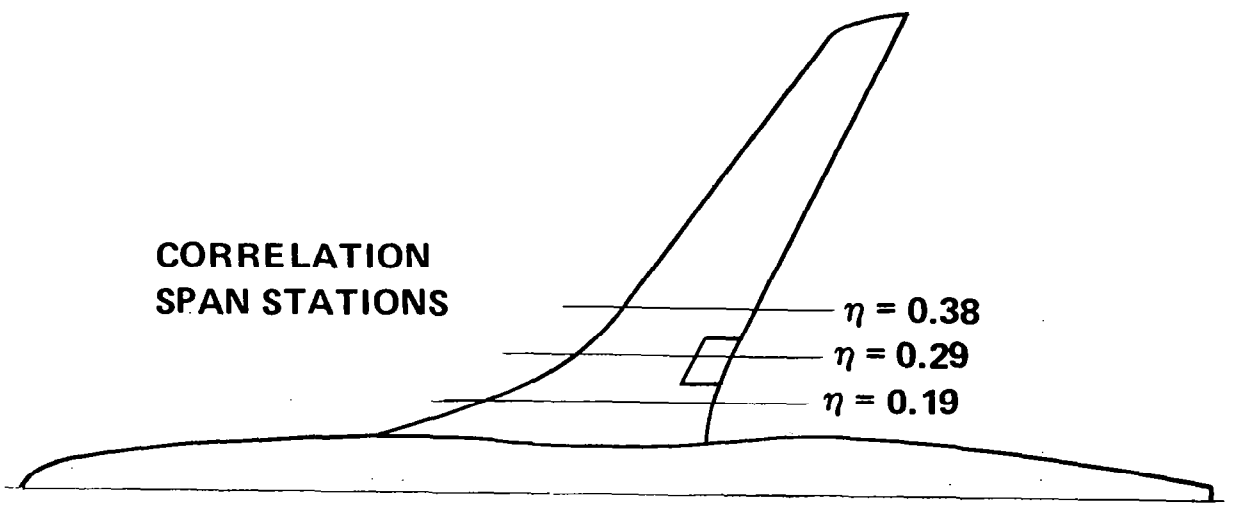

Figure 2.- Supercritical wing/area ruled fuselage transport configuration with control surface deflections (ref. 10).

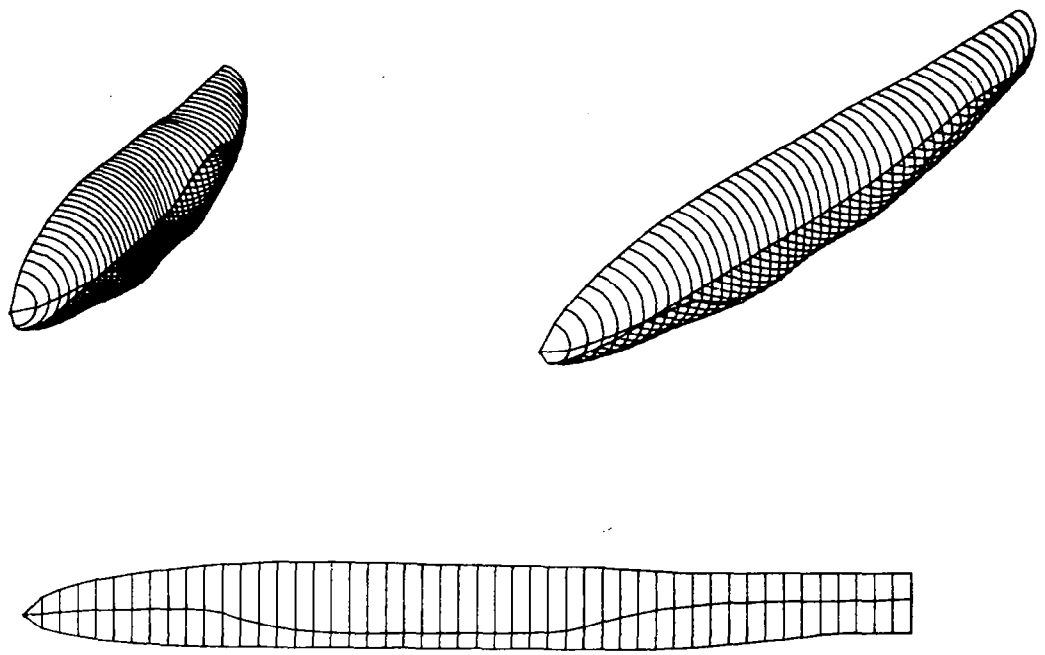

Figure 3.- Fuselage geometry math model (ref. 10.)

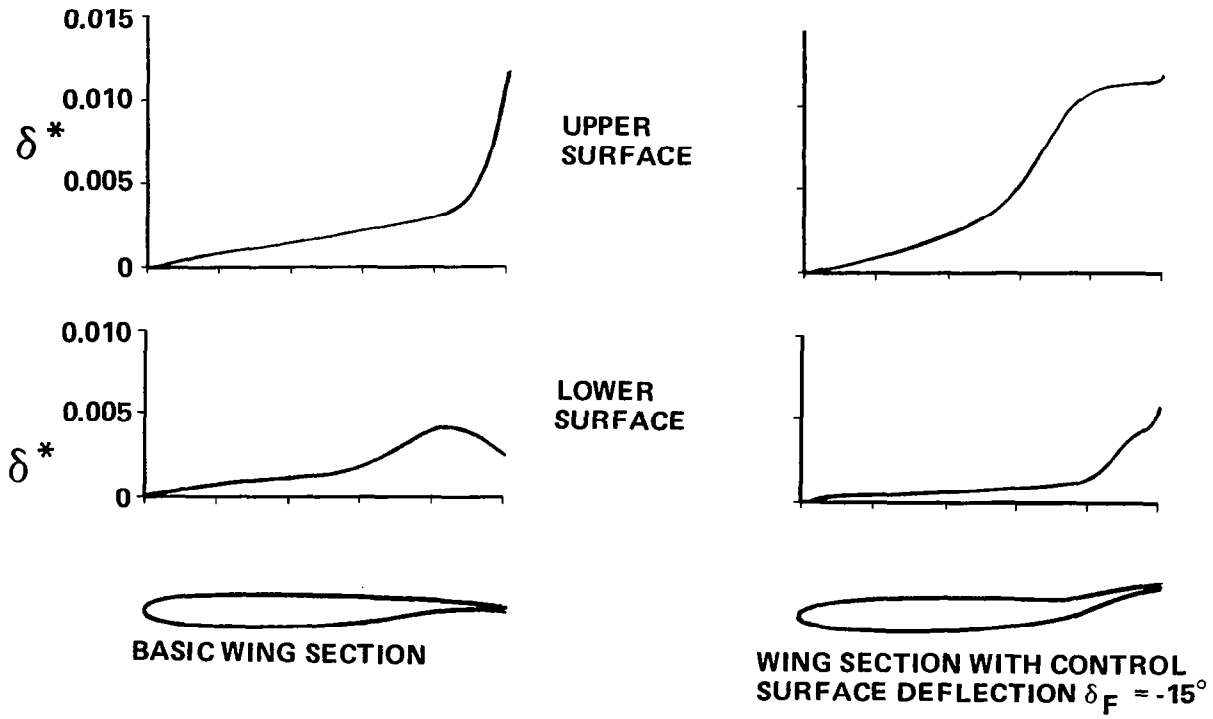

Figure 4.- Wing boundary layer displacement thickness at $\eta = 0.31$.

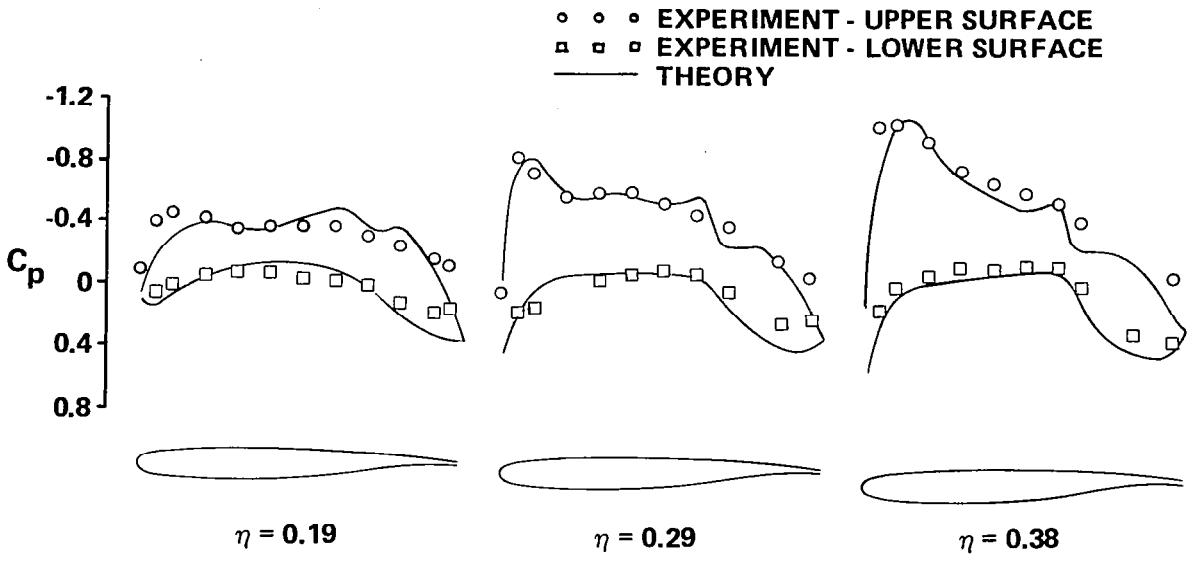

Figure 5.- Wing pressure distribution correlation (basic wing (ref. 10) $M_\infty = 0.9$, $\alpha = 3.91°$).

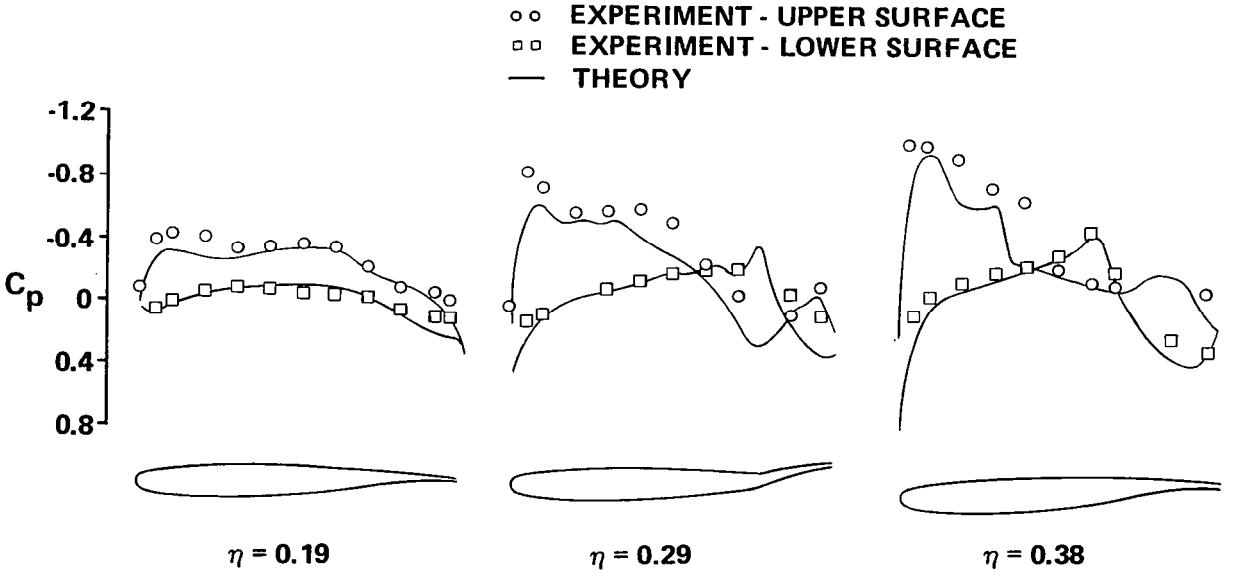

Figure 6.- Wing pressure distribution correlation (with wing control surface deflection (ref. 10) $\delta_F = -15°$, $M_\infty = 0.9$, $\alpha = 3.93°$).

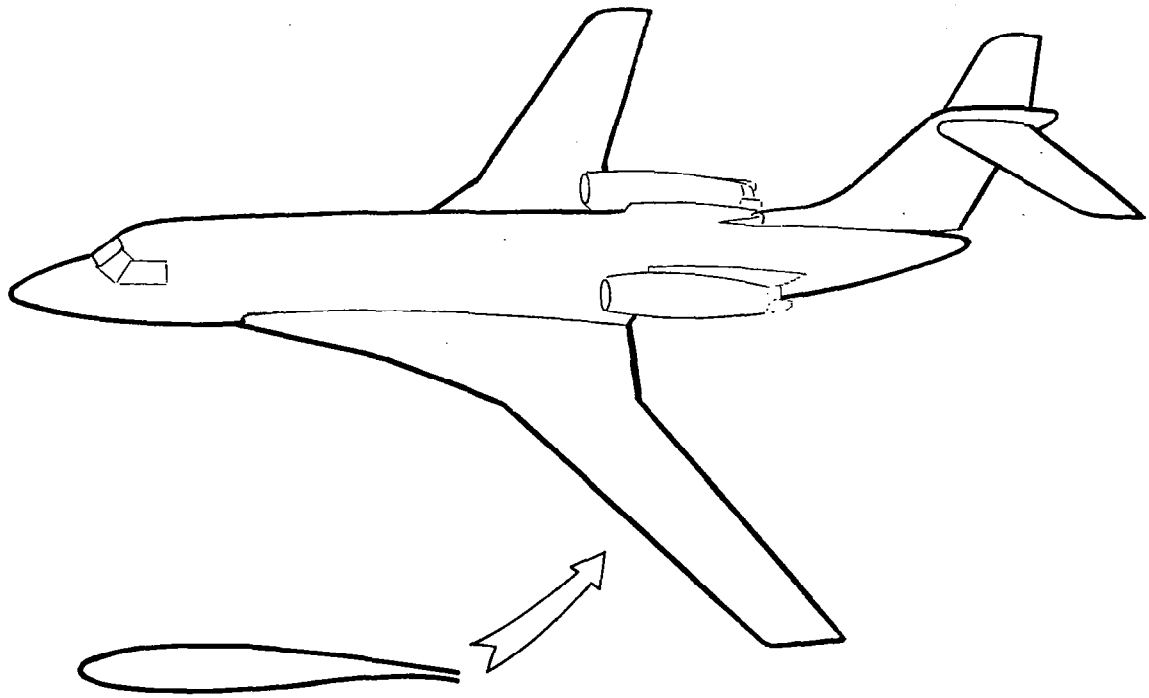

Figure 7.- Supercritical wing transport configuration.

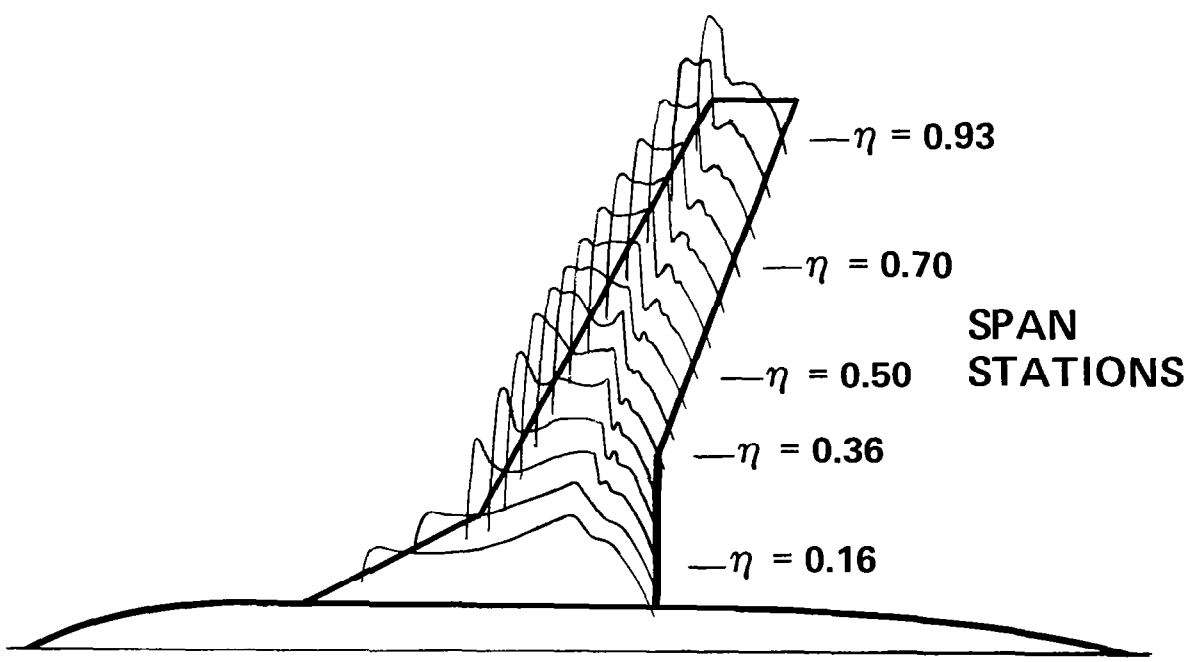

Figure 8.- Computed pressure distributions for supercritical wing transport, M = 0.825, $\alpha = 4^{\circ}$.

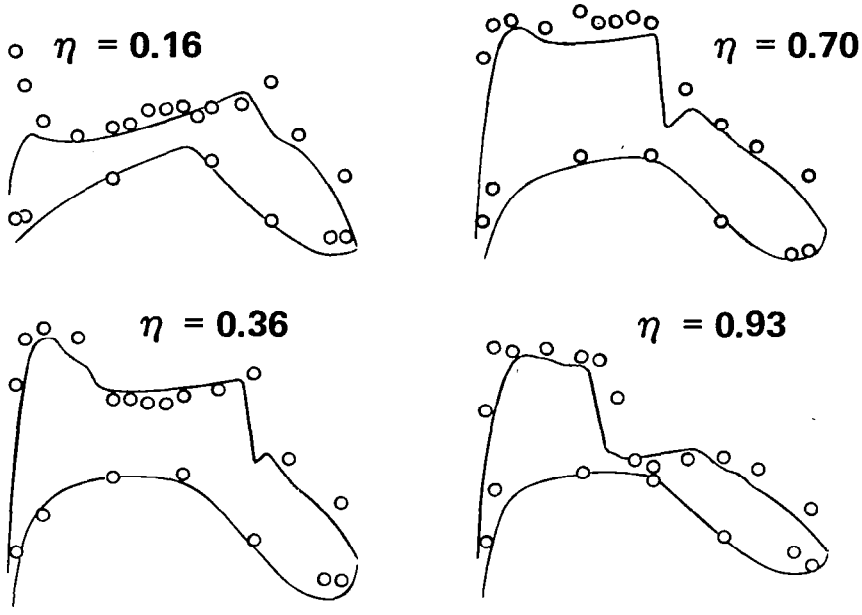

Figure 9.- Pressure distribution correlation for supercritical wing transport, M = 0.825, $\alpha = 4^\circ$.

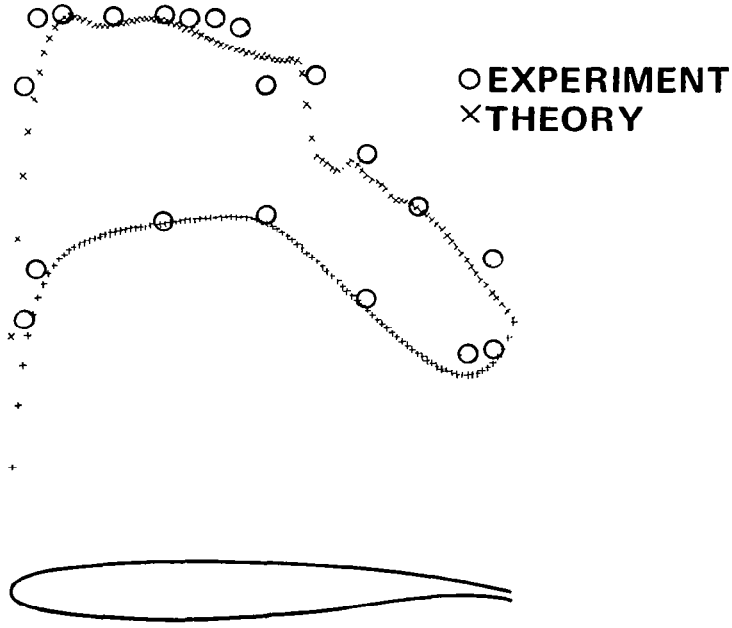

Figure 10.- Details of mid-span pressure distribution, M = 0.825, $\alpha = 4^\circ$.

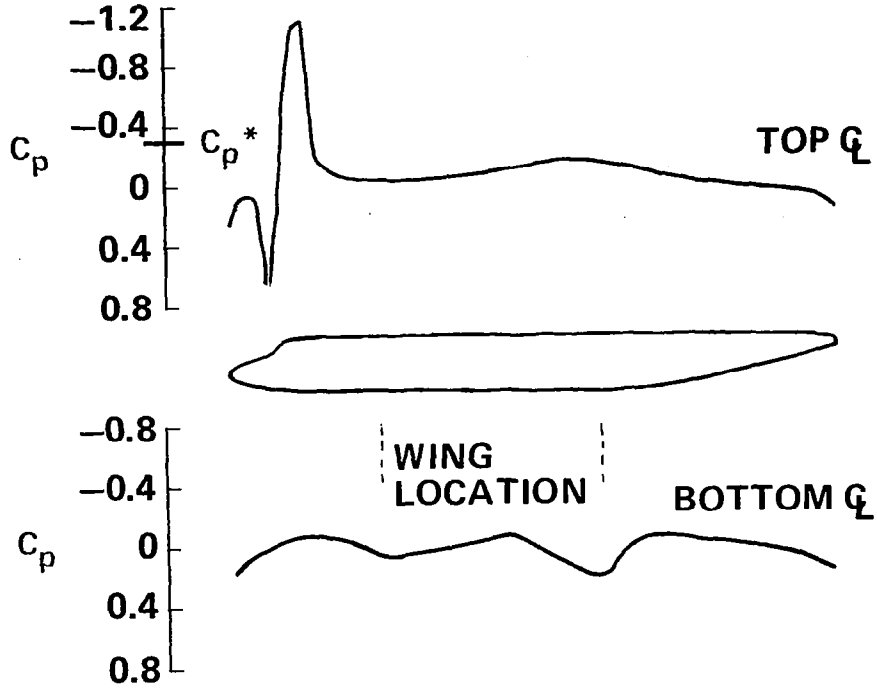

Figure 11.- Computed transport fuselage pressure distribution, $M = 0.825$, $\alpha = 4^{\circ}$.

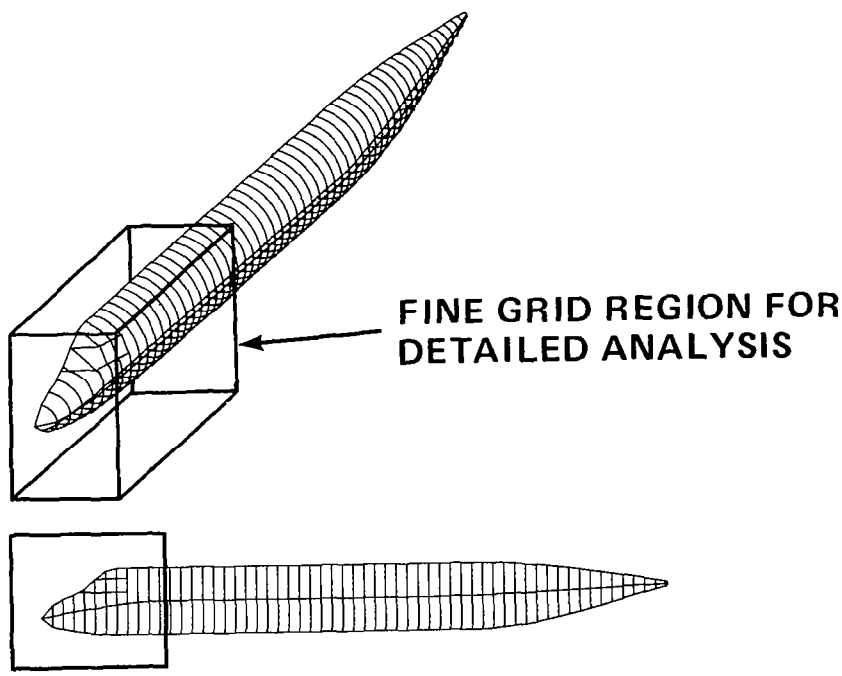

Figure 12.- Transport fuselage surface geometry.

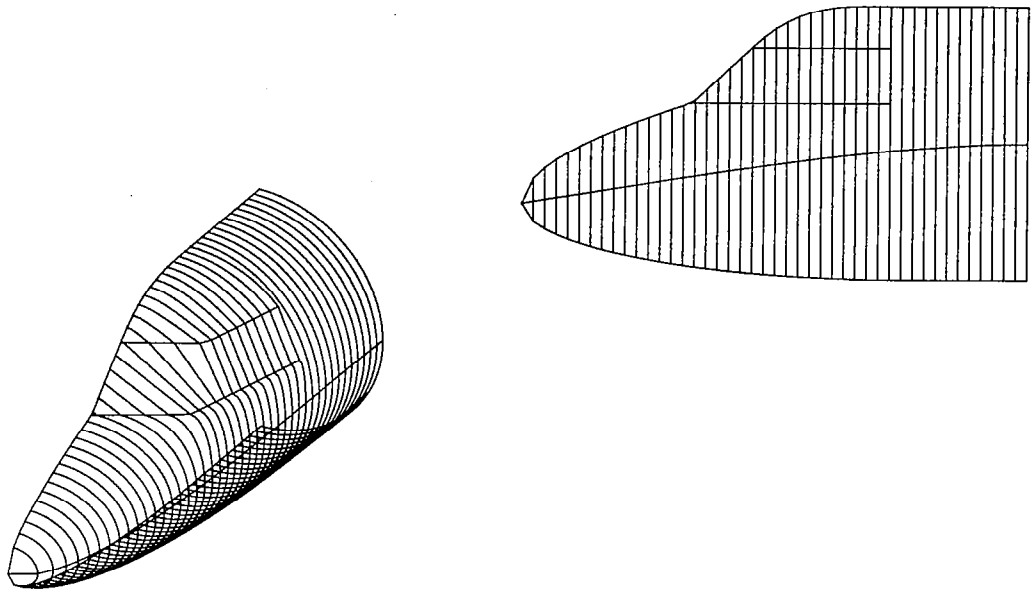

Figure 13.- Details of geometry for fine grid region.

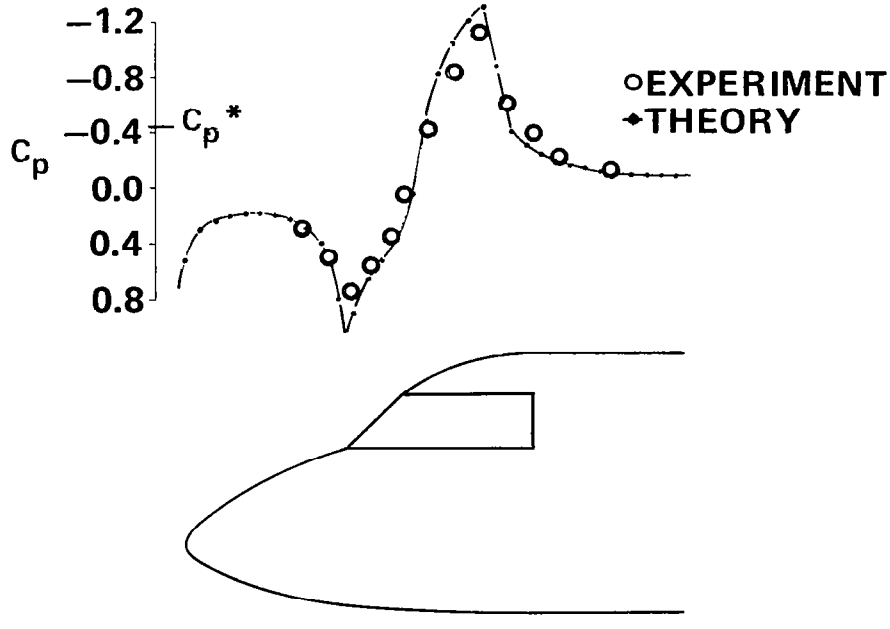

Figure 14.- Transport fuselage top centerline pressure distribution correlation, $M_\infty = 0.8$, $\alpha = 3.1°$.

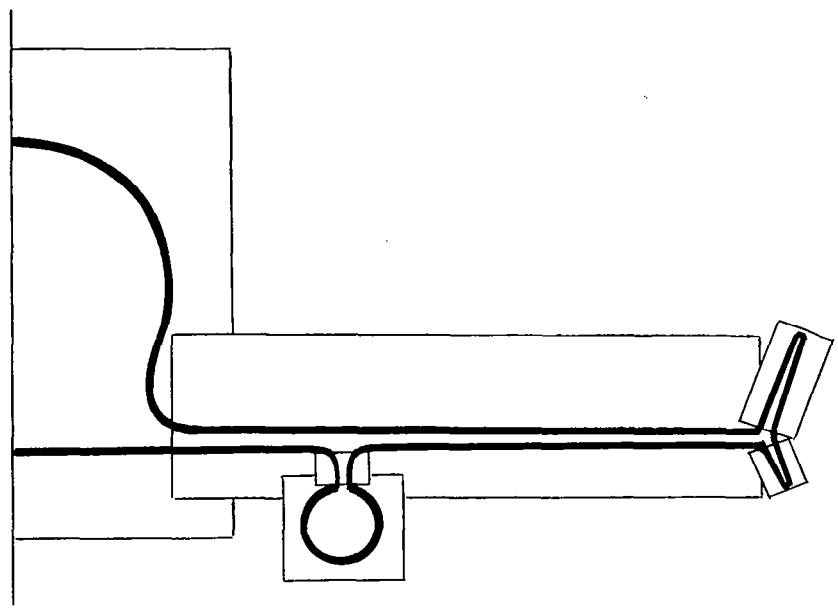

Figure 15.- Anticipated grid component build-up capability for complete configurations.

1. Report No.	2. Government Accession No.	3. Recipient's Catalog No.
NASA CR-3030		

4. Title and Subtitle	5. Report Date
TOWARDS COMPLETE CONFIGURATIONS USING AN EMBEDDED GRID APPROACH	July 1978
	6. Performing Organization Code

7. Author(s)	8. Performing Organization Report No.
Charles W. Boppe	

9. Performing Organization Name and Address	10. Work Unit No.
Grumman Aerospace Corporation Bethpage, NY 11714	516-53-01-13
	11. Contract or Grant No. NAS1-14732

12. Sponsoring Agency Name and Address	13. Type of Report and Period Covered
National Aeronautics and Space Administration Washington, DC 20546	Contractor Report
	14. Sponsoring Agency Code

15. Supplementary Notes

(a) This paper was presented at the CTOL Transport Technology Conference held at Langley Research Center on February 28 to March 3, 1978.

(b) Langley Technical Monitor: Perry A. Newman Final Report

16. Abstract

A new approach to simulating transonic flow about transport configurations is briefly outlined. The methods embedded grid scheme provides a high degree of computational resolution coupled with geometric flexibility for future applications to complex shapes. Calculations presented illustrate aspects of transonic transport design including fuselage design, determination of wing control surface deflection effectiveness, and wing design.

17. Key Words (Suggested by Author(s))	18. Distribution Statement
Aerodynamics Transonic flow Supercritical Wings	FEDD Distribution Subject Category 02

19. Security Classif. (of this report)	20. Security Classif. (of this page)	21. No. of Pages	22. Price*
Unclassified	Unclassified	16	$4.00

Available: NASA's Industrial Applications Centers

NASA-Langley, 1978